scientific reports

Check for updates

OPEN

Narrow tuning and sensitivity of the pheromone-specific olfactory neuron in male European grapevine moth (*Lobesia botrana*)

Zsolt Kárpáti[1,2]✉, Ferenc Deutsch[1], Benjamin Lőczi[1], Anna Teski[1], Adrien Fónagy[1], József Fodor[1], Virág Takács[3], Gabriella Köblös[1], Gábor Nyiri[3] & Júlia Katalin Jósvai[1]

The European grapevine moth (*Lobesia botrana*, Lepidoptera: Tortricidae) is a serious pest of grapevine. Understanding male peripheral detection of the female-produced sex pheromone is essential for improving pest management strategies. Yet, despite its importance, the functional properties and specificity of the pheromone-sensitive olfactory sensory neurons (OSNs), housed in *sensilla trichodea* in this species, remain incompletely characterized. Here, we used single sensillum recording (SSR) to systematically test the responses of male OSNs to 24 pheromone stimuli. The OSNs gave the most specific response to the major pheromone component, (E,Z)-7,9-dodecadienyl acetate (E7,Z9-12Ac), but (Z,Z)-7,9-dodecadienyl acetate (Z7,Z9-12Ac) also significantly excited the neuron in higher doses. The OSNs also responded to two other compounds, (Z)-9-dodecenyl acetate (Z9-12Ac) and (Z)-9-undecenyl acetate (Z9-11Ac), at the highest dose. The other two stereoisomers of the major pheromone component, E7,E9-12Ac and Z7,E9-12Ac did not elicit any response. Cross-adaptation experiments and electron microscopic study of sensillar morphology confirmed that only one neuron per sensillum mediates these responses, indicating narrow ligand specificity rather than strict, high specificity. In contrast, electroantennaography (EAG) recordings of whole antennal responses demonstrated a broadening of pheromone tuning specificity, suggesting that the integration of responses from different OSN types may contribute to this phenomenon.

Keywords *Lobesia botrana*, Pheromone, Single sensillum recording, Electroantennography, Cross-adaptation, Olfactory sensory neuron

The European grapevine moth (*Lobesia botrana*; Lepidoptera: Tortricidae) is a significant economic pest of grapevine (*Vitis vinifera*) in Europe, as well as in South and North American countries[1]. While the control of *L. botrana* is mainly based on insecticide treatments[2], in some countries these have been replaced by more selective and safer methods, such as mating disruption, which uses the major sex pheromone component of this species[1].

The main sex pheromone component produced by female *L. botrana* is (E,Z)-7,9-dodecadienyl acetate (E7,Z9-12Ac)[3,4]. In addition, minor pheromone components, including (E,Z)-7,9-dodecadien-1-ol (E7,Z9-12OH) and (Z)-9-dodecenyl acetate (Z9-12Ac), have been identified, which, combined with the main pheromone component, increased the male attraction in wind tunnel assays[5]. The addition of (E)-9-dodecenyl acetate (E9-12Ac) and Δ11-dodecenyl acetate (11-12Ac) to the previous three-component blend further increased male attraction[6]. Furthermore, detailed chemical and electrophysiological analysis of female pheromone gland extract demonstrated that combining (E)-7-dodecenyl acetate (E7-12Ac) and (E,Z)-7,9,11-dodecatrienyl acetate with the main component also enhanced male attraction in wind tunnel assays[7]. While adding these minor components attracts more males in laboratory assays, only E7,Z9-12Ac is utilised in the field for monitoring and mating disruption techniques.

In moths, the multi-component nature of pheromones requires highly specialszed sensory systems to accurately detect and differentiate these species-specific signals. The pheromone-sensitive olfactory sensory neurons (OSNs) housed in *sensilla trichodea* in the male antennae are highly abundant and sensitive to low

[1]Department of Chemical Ecology, Plant Protection Institute, HUN-REN Centre for Agricultural Research, Budapest, Hungary. [2]Department of Animal Ecology and Tropical Biology, University of Würzburg, BiocenterWürzburg, Germany. [3]Laboratory of Cerebral Cortex Research, HUN-REN Institute of Experimental Medicine, Budapest, Hungary. ✉email: karpati.zsolt@atk.hun-ren.hu

concentrations of pheromone components[8]. According to electrophysiological recordings, this type of sensilla usually contains 1–3 OSNs[9–11]. Typically, OSNs express a single type of olfactory receptor protein, following the 'one receptor per neuron' rule, which allows them to respond to specific ligands [12–15]. The pheromone receptor located on the OSN can be ligand-specific, narrowly or broadly tuned to pheromone-related stimuli[16]. The ligand-specific moth pheromone receptors are sensitive to only one compound, discriminating even subtle differences such as chain length, functional group, position of the double bond, or stereoisomeric differences[16–21]. Narrowly tuned pheromone receptors respond primarily to chemically similar compounds[22]. In contrast, broadly tuned receptors have a wider response spectrum and can detect chemically diverse pheromone compounds[11,23]. Additionally, there are numerous examples of single pheromone receptor neurons that can express more than one pheromone receptor protein[11,24].

The antennal morphology, including the presence of different sensilla types on the antennae of both males and females, has been studied in *L. botrana*[25]. Interestingly, this study showed that long *s. trichodea* type III was observed only on male antennae. Electroantennography (EAG), which detects summed antennal responses generated by activated olfactory sensory neurons, indicated that the male antenna of *L. botrana* responds strongly to the main pheromone component (E7,Z9-12Ac) but also showed a response, though weaker, to Z9-12Ac and E7,Z9-12OH[26].

Using the single sensillum recording (SSR) technique, Cristofaro[20] demonstrated that olfactory sensilla located on the male antenna can detect the E7,Z9-12Ac, the main pheromone component of this species; however, they did not specify which sensillum type was involved. Despite this, a comprehensive characterisation of the physiological response of pheromone receptor neurons in male *L. botrana* remains incomplete.

The three-dimensional neuroanatomical structure of the antennal lobe, the primary brain olfactory centre of *L. botrana*, shows that males possess a single macroglomerulus located close to the entrance of the antennal nerve, which may be responsible for the perception of the major pheromone component. However, no physiological evidence has been provided[28].

Despite previous studies on *L. botrana* antennal morphology and pheromone detection, the functional specificity and sensitivity of the pheromone-sensitive OSNs located in *sensilla trichodea* remain incompletely understood. We hypothesised that these sensilla house either one or more ligand-specific, narrowly or broadly tuned OSNs. By combining SSR and scanning electron microscopy (SEM), we aimed to characterise the physiological response and morphological structure of the pheromone-sensitive *s. trichodea* type III in male *L. botrana*.

Results

Tuning specificity of pheromone-sensitive OSNs

To characterise the response of the OSNs to various pheromone stimuli, we performed SSR from type III *s. trichodea* situated between the 5th and 28th segments of the male antenna, utilising 24 relevant synthetic stimuli with potential pheromonal activity (Table 1). Among the 24 tested compounds, only four elicited responses significantly stronger than the control (one-way ANOVA, $F_{24,822} = 38.68$, $p < 0.001$; Dunnett's post hoc test, $p < 0.05$). All 36 tested *s. trichodea* type III, irrespective of the position on the antenna, displayed the strongest response to the major pheromone component, E7,Z9-12Ac (Tukey's HSD post hoc test, $p < 0.05$; Fig. 1A, B). The second strongest response was evoked by Z7,Z9-12Ac. Gas chromatography (GC) coupled with electroantennographic detection (GC-EAD) confirmed that antennal responses were elicited only by the main Z7,Z9-12:Ac peak and not by E7,Z9-12Ac impurity, indicating that the EZ isomer did not cause any false positive responses (Fig. S1). This type of sensillum also responded to Z9-11Ac and Z9-12Ac, though less strongly than to the major component or Z7,Z9-12Ac (Fig. 1A). Interestingly, the other two isomers of the major pheromone component (E7,E9-12Ac and Z7,E9-12Ac) did not elicit any response. Similarly, none of the other 18 tested pheromone compounds evoked a response stronger than the control stimulus (Fig. 1A). The spontaneous activity of the tested neurons ranged from 0 to 32 Hz. After or during stimulation, there was no evidence of inhibitory responses (decreased spike frequency compared to spontaneous activity) of OSNs. Regarding the latencies, one-way ANOVA indicated a significant effect of the investigated compounds on response latency ($F_{3,104} = 3.41$, $p < 0.05$); however, post-hoc pairwise comparisons did not reveal significant differences between the four compounds, which elicited stronger responses than the control stimulus (Tukey HSD, $p > 0.05$ for all comparisons (Fig. 1B).

Sensitivity of pheromone-sensitive OSN

To analyse the sensitivity of the OSN located in the sensillum, we performed dose–response studies using four different doses (10^1–10^4 ng) of the four previously mentioned active pheromone components (E7,Z9-12Ac, Z7,Z9-12Ac, Z9-12Ac, and Z9-11Ac; Fig. 2A, B). The overall one-way ANOVA conducted on raw data revealed significant differences among the tested stimuli ($F_{16,155} = 31.19$, $p < 0.001$). At the lowest dose (10^1 ng), neither of the compounds elicited a higher spike number than the control stimuli (Dunnett's post hoc test, $p > 0.05$) and no significant differences were observed among compounds (one-way ANOVA, $F_{3,31} = 0.442$, $p = 0.725$). At a dose of 10^2 ng, only E7,Z9-12Ac, the major pheromone component, evoked a significantly greater response compared to the control (Dunnett's post hoc test, $p < 0.05$), while the other three compounds did not. At the 10^3 ng dose, both E7,Z9-12Ac and Z7,Z9-12Ac elicited a significantly stronger responses than the control (Dunnett's post hoc test, $p < 0.05$); however, when comparing the two compounds, E7,Z9-12Ac gave a significantly stronger response (one-way ANOVA, $F_{3,31} = 16.46$, $p < 0.001$, Tukey's HSD test). At the highest tested dose (10^4 ng), all tested compounds elicited significantly stronger responses compared to the control (Dunnett's post hoc test, $p < 0.05$) and no significant differences were found among the compounds (one-way ANOVA, $F_{3,13} = 1.656$, $p = 0.197$; Fig. 2A). Responses to all tested compounds increased with dose. Pearson correlation analysis revealed strong positive correlations between dose and normalized spike number for E7,Z9-12Ac ($r(34) = 0.79$, $p < 0.001$),

Tested compounds	Abbreviations	CAS	Source	Purity %	Chemical class	Function*	References
(E,Z)-7,9-dodecadienyl acetate	E7,Z9-12Ac	55,774–32-8	Pherobank	89.9	ester	A	47
(E,Z)-7,9-dodecadien-1-ol	E7,Z9-12OH	54,364–60-2	BASF	~90.0	alcohol	B	5
(Z)-9-dodecenyl acetate	Z9-12Ac	16,974–11-1	Pherobank	99	ester	B	5
(E)-7-dodecenyl acetate	E7-12Ac	16,695–41-3	Farchan	99	ester	B	7
(E)-9-dodecenyl acetate	E9-12Ac	35,148–19-7	Pherobank	99	ester	B	6
Δ11-dodecenyl acetate	11-12Ac	35,153–10-7	Pherobank	97	ester	B	6
(E,E)-7,9-dodecadienyl acetate	E7,E9-12Ac	54,364–63-5	Pherobank	98.8	ester	C	7
(Z,Z)-7,9-dodecadienyl acetate	Z7,Z9-12Ac	67,818–23-9	Pherobank	97.8	ester	C	7
(Z,E)-7,9-dodecadienyl acetate	Z7,E9-12Ac	–	Pherobank	95.9	ester	C	7
octadecyl acetate	18Ac	822–23-1	Pherobank	99	ester	C	5
(Z)-9-dodecen-1-ol	Z9-12OH	35,148–18-6	Farchan	99.9	alcohol	C	48
tetradecyl acetate	14Ac	638–59-5	Pherobank	99	ester	C	7
octadecan-1-ol	18OH	112–92-5	Pherobank	99	alcohol	C	7
eicosan-1-ol	20OH	629–96-9	Merck	98	alcohol	C	7
dodecyl acetate	12Ac	112–66-3	Pherobank	99	ester	C	7
(E)-9-dodecen-1-ol	E9-12OH	35,237–62-8	Pherobank	98.8	alcohol	C	49
decyl acetate	10Ac	112–17-4	Pherobank	98.7	ester	C	5
hexadecyl acetate	16Ac	629–70-9	Pherobank	99	ester	C	50
(E)-9,11-dodecadienyl acetate	E9,11-12Ac	50,767–78-7	Pherobank	96	ester	C	51
(Z)-9-undecenyl acetate	Z9-11Ac	85,576–13-2	Pherobank	99	ester	C	52
(Z)-10-tridecenyl acetate	Z10-13Ac	64,437–24-7	Pherobank	99	ester	C	53
(Z)-11-tetradecenyl acetate	Z11-14Ac	20,711–10-8	Pherobank	99	ester	C	54
(E)-11-tetradecenyl acetate	E11-14Ac	33,189–72-9	Pherobank	99	ester	C	54
(Z)-11-tetradecen-1-ol	Z11-14OH	34,010–15-6	Pherobank	98	alcohol	C	55

Table 1. Classifications, origins, and functions of the tested pheromone-related compounds used in the study. * A—major pheromone component of *Lobesia botrana*; B—minor pheromone component of *Lobesia botrana*; C—putative pheromone components of closely related species.

Z7,Z9-12Ac ($r(34) = 0.71$, $p < 0.001$), moderate positive correlations for Z9-11Ac ($r(34) = 0.62$, $p < 0.001$) and Z9-12Ac ($r(34) = 0.56$, $p < 0.001$) (Fig. 2A).

Cross-adaptation

We performed a cross-adaptation experiment using the SSR setup to determine whether a single OSN located in the *s. trichodea* type III can detect two different pheromone compounds (E7,Z9-12Ac and Z7,Z9-12Ac), or whether two separate neurons within the same sensillum are responsible for detecting the different isomers. Comparing the spike numbers elicited by the first and second stimulus within each sequence, the cross-adaptation test showed that *s. trichodea* type III does not respond to the second stimulus in any of the tested combinations (Fig. 3A, B). Paired *t*-tests confirmed a significant reduction in response to the second stimulus compared to the first in all tested combinations ($t_8 = 14.0$, $p < 0.001$ for E7,Z9-12Ac → E7,Z9-12Ac; $t_9 = 11,7$, $p < 0.001$ for E7,Z9-12Ac → Z7,Z9-12Ac; $t_6 = 6.01$, $p < 0.001$ for Z7,Z9-12Ac → E7,Z9-12Ac and $t_8 = 9.2$, $p < 0.001$ for Z7,Z9-12Ac → Z7,Z9-12Ac; Fig. 3A).

Serial section scanning electron microscopy (ssSEM)

To confirm that *s. trichodea*, tested in SSR and cross-adaptation experiments, housing only one dendrite inside the sensillum, we carried out electron microscopy experiments. *S. trichodea* profiles were identified in consecutive serial electron microscopic section series based on the absence of a socket at their point of origin and the presence of a thick cuticle covered with pores[25]. This represented the most frequently observed sensilla type. We traced individual *s. trichodea* through consecutive ssSEM images. We found only one dendrite in 44 out of 45 sensilla trichodea (from n = 2 moths). The remaining 1 sensillum contained more than one dendrite, but it was technically not possible to determine whether they originated from a single neuron or from separate cells. (Fig. 5).

Electroantennography (EAG)

We used EAG recordings from the entire male antenna of *L. botrana*, including all sensilla, to assess sensitivity to the four above-mentioned active pheromone stimuli (E7,Z9-12Ac, Z7,Z9-12Ac, Z9-12Ac, and Z9-11Ac), creating dose–response curves of each compound (Fig. 4A, B).

The overall one-way ANOVA conducted on these data revealed significant differences among the tested stimuli ($F_{16,153} = 15.81$, $p < 0.001$). At the two lowest doses (10^1 and 10^2 ng) the responses to the tested compounds did not differ from the control (Dunnett's post hoc test, $p > 0.05$) nor did they differ from each other (one-way ANOVA, $F_{3,36} = 1.334$, $p = 0.279$ for 10^1 ng and $F_{3,36} = 0.128$, $p = 0.943$ for 10^2 ng, respectively). At a dose of 10^3 ng,

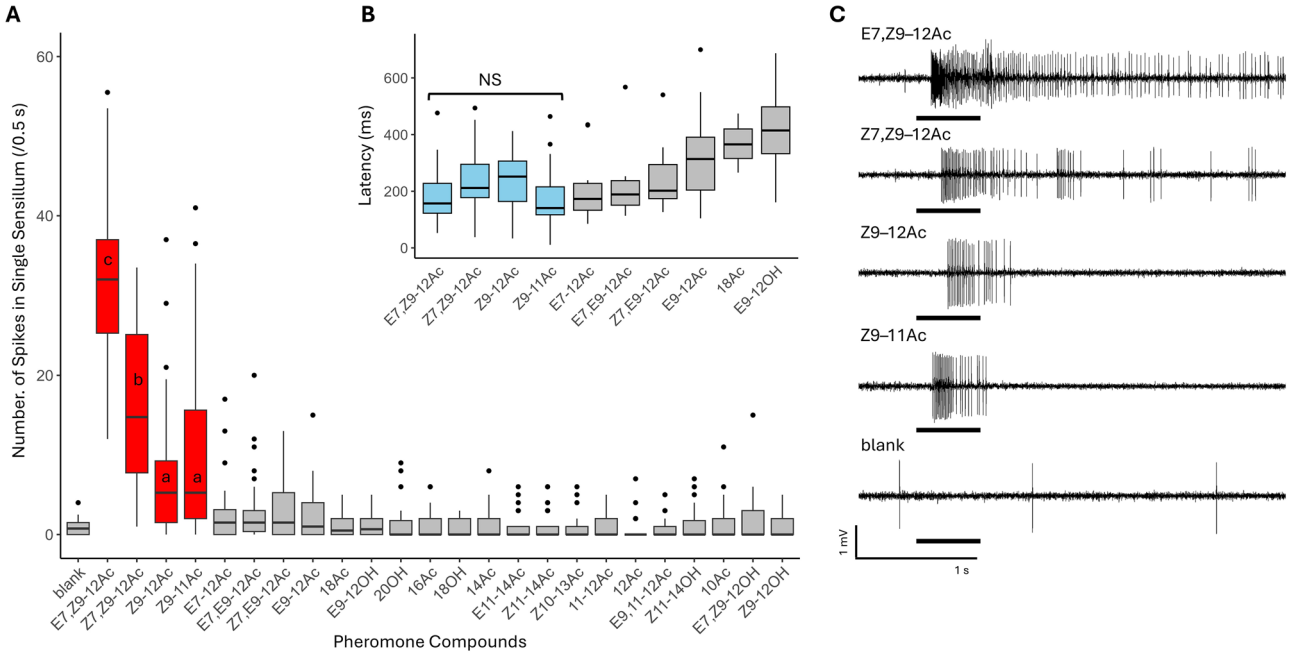

Fig. 1. Single sensillum electrophysiological recordings from *s. trichodea* type III in male *L. botrana*. (A) Boxplot showing the number of spikes elicited by different tested compounds over 0.5 s. The stimulus load was 10^4 ng (n = 36). Active compounds that elicited stronger responses than the control stimulus (*n*-hexane) are highlighted in red (Dunette's test, $p < 0.05$). Statistical comparisons among active compounds were performed using ANOVA followed by Tukey's HSD test; responses marked with the same letter do not differ significantly ($p < 0.05$). (B) Boxplot illustrating response latency (ms) for compounds with measurable responses. Statistical evaluation was conducted only for compounds highlighted in blue, which elicited significantly stronger responses than the control (one-way ANOVA, Tukey's HSD test). NS, not significant (C) Representative single-sensillum recordings (SSRs) showing neuronal activity in response to selected active pheromone components and the control (blank). The horizontal bars under each recording represent stimulus duration (0.5 s).

both E7,Z9-12Ac and Z7,Z9-12Ac elicited a higher response than the control stimulus (Dunnett's post-hoc test, $p < 0.05$) and there was no significant difference between E7,Z9-12Ac and Z7,Z9-12Ac; however, E7,Z9-12Ac, elicited a significantly stronger response than Z9-12Ac and Z9-11Ac (one-way ANOVA, $F_{3,36} = 5.211$; $p = 0.004$). At the highest dose (10^4 ng), all compounds elicited a significantly stronger response compared to the control (Dunnett's post hoc test, $P < 0.05$) and the antenna responded equally strongly to E7,Z9-12Ac; Z7,Z9-12Ac and Z9-12Ac but not to Z9-11Ac (one-way ANOVA, $F_{3,36} = 14.9$, $p < 0.001$; Fig. 4). Responses to all compounds were dose-dependent, with significant positive correlations observed between dose and response for each compound ($r(38) = 0.680$, $p < 0.001$ for E7,Z9-12Ac; $r(38) = 0.685$, $p < 0.001$ for Z7,Z9-12Ac; $r(38) = 0.474$, $p < 0.05$ for Z9-11Ac; and $r(38) = 0.687$, $p < 0.0001$ for Z9-12Ac) (Fig. 4A).Overall, EAG recordings showed that the pheromone tuning specificity of the whole antenna, compared to the *s. trichodea* type III, was broadened at the 10^3 ng dose, as the antenna responded equally to both E7,Z9-12Ac and Z7,Z9-12Ac at this concentration.

Discussion

In this study, 24 different candidate pheromone compounds (Fig. 1, Table 1) were tested to characterise the physiological responses of male *L. botrana* OSNs housed in *s. trichodea* type III. This exists only on the male antenna and supposedly detects female-produced pheromone compounds[25]. When investigated with SSR, all tested *s. trichodea* responded strongly to the major pheromone component (E7,Z9-12Ac), consistent with a previous work showing that the olfactory sensilla of male *L. botrana* detected this component; however, that study did not specify which sensillum type was responsible for the detection[27]. The second strongest response was elicited by Z7,Z9-12Ac, a stereoisomer of the major pheromone component of this species. This compound has been found in trace amounts in the female pheromone gland, indicating that it is produced; however, male antennal detection or behavioural response has not been demonstrated[5,7]. Nevertheless, the other two stereoisomers of the major pheromone component, E7,E9-12Ac and Z7,E9-12Ac did not elicit any response in this neuron. Based on these results, we hypothesise that the olfactory receptor displays partial stereoisomer specificity. The same sensilla could respond to two additional components, Z9-12Ac and Z9-11Ac, which were previously identified as pheromone components of *L. botrana* and *Eupoecilia ambiguella*, respectively[5,29]. However, the spike frequency was lower compared to the major pheromone component (E7,Z9-12Ac) and the Z7,Z9-12Ac (Fig. 1A). These findings indicate that OSNs exhibit broader and hierarchical tuning but still narrow ligand specificity, even though they can detect more than one compound. A similar phenomenon has been observed in another moth species, *Ostrinia furnacalis*, where the same sensillum is capable of detecting

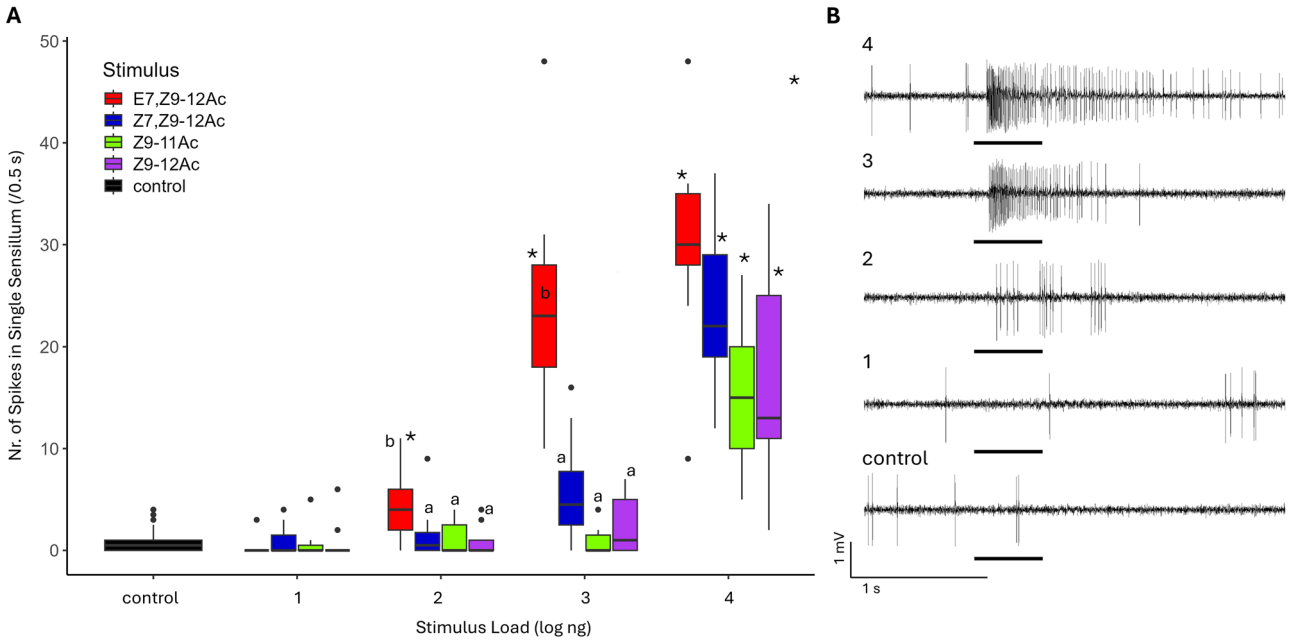

Fig. 2. Dose–response curves of pheromone-sensitive OSNs located in *s. trichodea* type III of male *L. botrana*. (**A**) Mean spike numbers (± SD) normalised to the control stimulus (*n*-hexane) elicited by four selected pheromone-related compounds (E7,Z9-12Ac (n = 9), Z7,Z9-12Ac (n = 10), Z9-12Ac (n = 9) and Z9-11Ac (n = 7)) in four doses (10^1–10^4 ng) over 0.5 s. Where the responses differ significantly (at doses 10^2 and 10^3 ng), different letters show significant differences within the group (ANOVA, followed by Tukey's HSD post-hoc test, $p < 0.05$). Asterisks indicate responses significantly different from control stimuli (Dunnett's post-hoc test, $p < 0.05$). (**B**) Representative single-sensillum recordings showing neuronal activity in response to different doses of E7,Z9-12Ac (1, 2, 3 and 4 log ng) and the control.

two pheromone components, E12- and Z12-tetradecenyl acetate[30]. The olfactory system could detect a range of conspecific signals while prioritising the major component for behavioural activation[31]. Additionally, it is also possible that different types of sensilla are more specific to other compounds[22].

The SSR dose–response curves of these four tested compounds (E7,Z9-12Ac, Z7,Z9-12Ac, Z9-12Ac and Z9-11Ac) show a dose-dependent response, confirming that OSNs have different sensitivity to these compounds. The major pheromone component (E7,Z9-12Ac) elicited a response even at a low dose (10^2 ng), suggesting that this sensilla type is highly sensitive to this component. Such a high sensitivity to the major pheromone component was also observed at this dose using SSR in other tortricid and crambid species[32,33]. At higher doses, the OSN responded to other compounds, Z7,Z9-12Ac, Z9-12Ac and Z9-11Ac, indicating that while the neuron exhibits high specificity for the major pheromone component at low concentrations, its sensitivity broadens to include other related compounds as the concentration increases. Consistent with our findings, the responses of the moth, *Ostrinia scapularis* OR4 receptor to the sex pheromone components were also dose-dependent, showing clear differences in sensitivity to ligands in the order, E11-14Ac > Z11-14Ac > Z9-14Ac[20]. A further investigation on the moth *Helicoverpa assulta* revealed that a single, narrowly tuned OSN can also detect more than one pheromone component[22]. This neuron exhibits a strong response to the major pheromone component of the species but also shows a weaker response to another pheromone compound[22]. This suggests a potential overlap in their signalling pathways or receptor affinities, implying that these compounds may activate similar neural circuits.

The cross-adaptation experiment suggests that only one OSN, located in the sensillum is responsible for detecting both isomers and consequently the other 2 compounds, as adaptation to the first stimulus diminishes sensitivity to the second one (Fig. 3A). The electron microscopy data also support that these sensilla do not house additional OSNs (Fig. 5). In several other Lepidoptera species, this type of sensillum bears more than one OSN, where different ligand-specific neurons respond to different pheromone compounds, including pheromone antagonists[11,33,39]; however, there are also instances where this sensillum type houses only a single OSN[40,41].

The narrow tuning observed in our study, despite a lack of strict ligand specificity, is remarkable, as pheromone-sensitive OSNs usually exhibit high ligand specificity, i.e., they are finely tuned to one pheromone compound and are able to detect it with extreme sensitivity[34,35]. However, several studies have shown that pheromone-sensitive OSNs in moths can respond to multiple components[11,36,37]. For instance, in the oriental fruit moth, *Grapholita molesta*, another tortricid species, the OSN sensitive to the minor pheromone component is also capable of detecting the major one[24]. Furthermore, a single OSN can express as many as five olfactory receptors, contradicting the established principle of one olfactory receptor per OSN[11]. The co-expression of multiple olfactory receptors on a single neuron may play a key role in assisting heterospecific chemical communication in moths. In our case, we hypothesise that a single OSN located in the sensillum is narrowly tuned, not in the

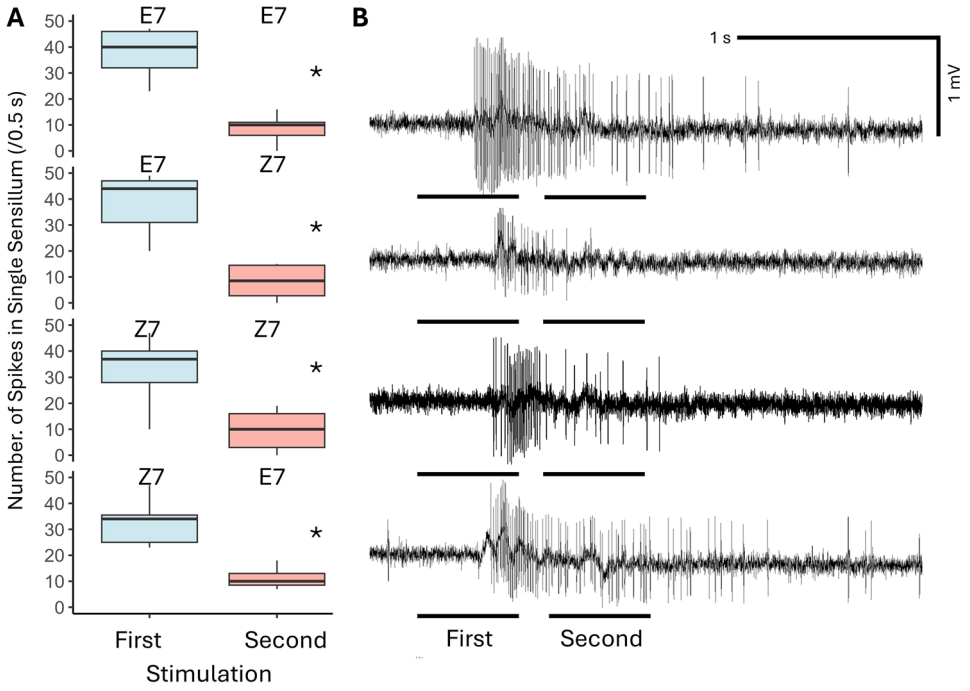

Fig. 3. Cross-adaptation test of pheromone sensitive OSNs in male *L. botrana* to consecutive 500 ms stimuli of selected pairs of the two sex pheromone components, E7,Z9-12Ac (E) and Z7,Z9-12Ac (Z) (**A**) Boxplots showing the number of spikes elicited by the first and second stimuli in each cross-adaptation pair (E7,Z9-12Ac and E7,Z9-12Ac – n = 9; pair of E7,Z9-12Ac and Z7,Z9-12Ac – n = 10; pair of Z7,Z9-12Ac and Z7,Z9-12Ac – n = 7; pair of Z7,Z9-12Ac and E7,Z9-12Ac – n = 9). Asterisks indicate significant differences in spike numbers between the two consecutive stimuli (paired *t*-test, $p < 0.05$). (**B**) Representative single-sensillum recordings illustrating neuronal activity to the consecutive stimuli.

sense of being specific for a single ligand, but rather in its ability to detect structurally similar compounds. This nuanced form of tuning differs from the strict specificity observed in many other moth species[38]. Such findings highlight the complexity of pheromone communication and raise questions about how insects might integrate multiple signals.

The broadening of pheromone tuning specificity observed in EAG recordings is likely influenced by the integration of signals from different types of OSNs. However, since EAG measures the combined response of the entire antenna, it is not possible to determine the precise contribution of each OSN type from these data alone. Therefore, although the results suggest that multiple OSN types may contribute to the broadened response, this conclusion remains tentative.

Future studies should focus on investigating the physiological responses of different types of sensilla to identify which specific sensilla are responsible for detecting other already identified minor pheromone components, such as E7,Z9-12OH and E7-12Ac. Additionally, researchers could employ various behavioural assays and field tests to correlate these physiological responses with actual insect behaviour, including Z7,Z9-12Ac as a potentially new minor pheromone component. Molecular approaches, including pheromone receptor gene expression analysis, as well as anatomical studies tracing OSN projections to the macroglomerular complex in the antennal lobe, would provide a deeper understanding of the sensory mechanisms involved. Understanding these mechanisms may provide better insights into the chemical communication of *L. botrana* and enhance pest management strategies.

Materials and methods

Insects

The adults of the European grapevine moth (*Lobesia botrana*) were collected near Trento, Italy. The moths were reared in the laboratory, and the culture was maintained on a semi-artificial diet[42] at 24 °C, 60% RH under 16:8 L:D light conditions. Pupae were sexed and separated in glass containers. Adults were fed with 5% honey water. Unmated, 1–4-day-old males were used for all experiments.

Pheromone stimuli

Twenty-four candidate pheromone compounds were chosen for the experiments based on literature data (Table 1). Each synthetic compound was dissolved in *n*-hexane (CAS: 110-54-3; Carl Roth GmBH, Karlsruhe, Germany). For the initial dilution, 10 µl of the pure compound was mixed with 990 µl of n-hexane to obtain a 10 µg/µl solution. To prepare a 1 µg/µl dilution, 100 µl of the 10 µg/µl solution was added to 900 µl of n-hexane. This serial dilution protocol was repeated as needed to achieve lower concentrations. Ten µl of the corresponding dilutions

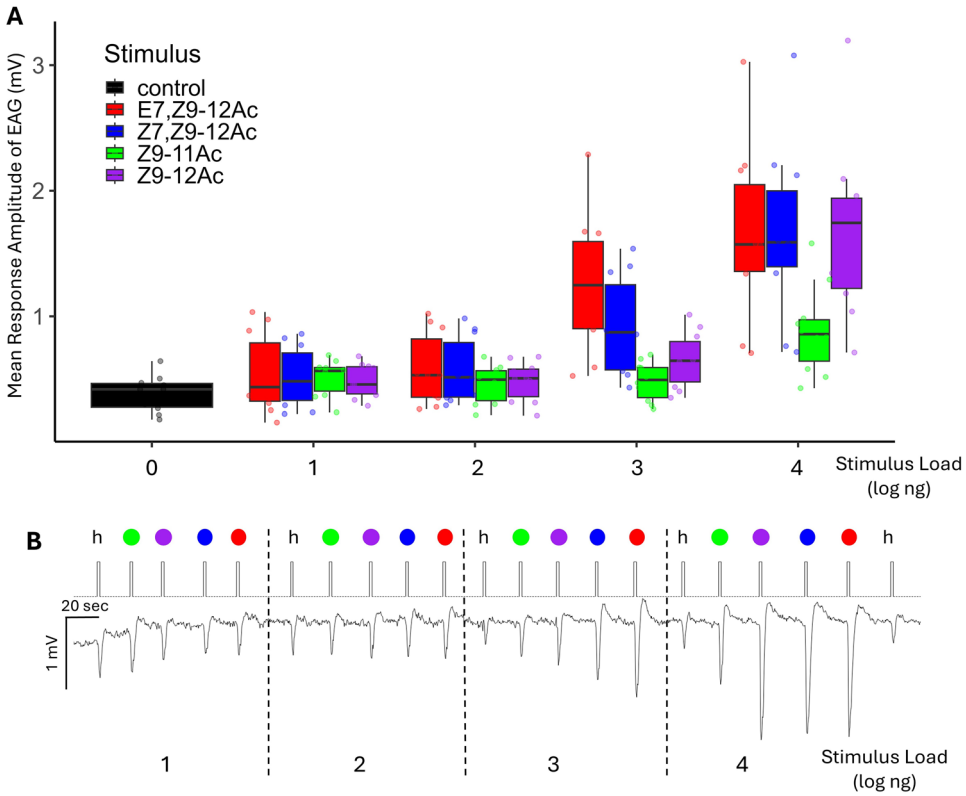

Fig. 4. Dose–response curves of EAG recordings of male *L. botrana* for selected test compounds (**A**) Boxplots showing antennal responses normalised to the control stimulus (*n*-hexane) elicited by four selected compounds at four different doses (n = 10). Responses within each dose group marked with the same letter do not differ significantly (ANOVA, followed by Tukey's HSD test, $p < 0.05$). Asterisks indicate responses significantly different from control stimuli (Dunnett's post-hoc test, $p < 0.05$). (**B**) Representative antennal responses to the synthetic pheromone-related compounds in the four different doses and *n*-hexane (h) as control stimuli.

(1, 10, 100, 1000 ng/µl) of the compounds were deposited on a filter paper disk (12.7 mm Ø; Schleicher & Schnell GmbH, Dassel, Germany), which was previously placed into a Pasteur pipette and used as a stimulus cartridge in the experiments. Gas chromatographic analysis (Agilent 6890N gas chromatograph; Agilent Technologies Inc., Santa Clara, CA, USA) showed that Z7,Z9-12Ac contained 0.6% E7,Z9-12Ac as a contaminant (see details in Fig. S1).

Single sensillum recordings

To characterise which pheromone compounds can be detected by *s. trichodea* type III, we performed SSR with sharp tungsten electrodes using standard equipment (Ockenfels Syntech, Buchenbach, Germany). The male was inserted into a plastic micropipette tip to immobilise the body. The head protruded from the tip and was fixed with dental wax (Surgident periphery wax, Heraeus Kulzer GmbH, Hanau, Germany). Antennae were placed on a microscope glass slide covered with inert glue (Tanglefoot, Planet Natural Ltd., Bozeman, MT, USA). A sharpened tungsten wire reference electrode was inserted into the abdomen. The *s. trichodea* type III on the immobilised antenna was localised under a light microscope (Olympus BX51WI) based on the morphological criteria[25] at 750 × magnification. The electrolytically sharpened tungsten recording electrode was inserted into the base of the sensillum (Fig. S2) using a micromanipulator (DC-3 K, Märzhäuser-Wetzlar Gmbh & Co Kg, Wetzlar, Germany). The extracellular analogue signal originating from the OSNs was 10 × amplified using a pre-amplification probe (Universal Single Ended AC/DC Probe PRS-1, Ockenfels Syntech). The amplified signal was filtered with 50–60 Hz suppression and sampled at the rate of 9600 sample/s using an integrated digital–analogue converter (IDAC-4, Ockenfels Syntech) connected to a computer.

The antenna was placed in a charcoal-filtered, humidified air stream (1 L min^{-1}) via a glass tube (17 cm length × 7 mm ID) positioned 2 cm from the antenna. The 0.5-s-long stimuli (1 L min^{-1}) were delivered into the continuous air stream using a stimulus controller (CS-55, Ockenfels Syntech). A 10^4 ng dose was used to screen 24 different synthetic stimuli on 36 s. *trichodea* type III from different males. For the dose–response experiments, we tested doses of 10^1–10^4 ng on different males, focusing on *s. trichodea* type III, for four candidate compounds: E7,Z9-12Ac (n = 9), Z7,Z9-12Ac (n = 10), Z9-11Ac (n = 7), Z9-12Ac (n = 9). *N*-hexane, the solvent of the test compounds, was used as a control stimulus. The action potentials were recorded for 7 s, starting 1 s before the stimulus onset. The action potential spikes were counted manually 0.5 s before and 0.5 s after the stimulus onset. The spike number before the stimulus onset represents the spontaneous activity of the neuron. The spike

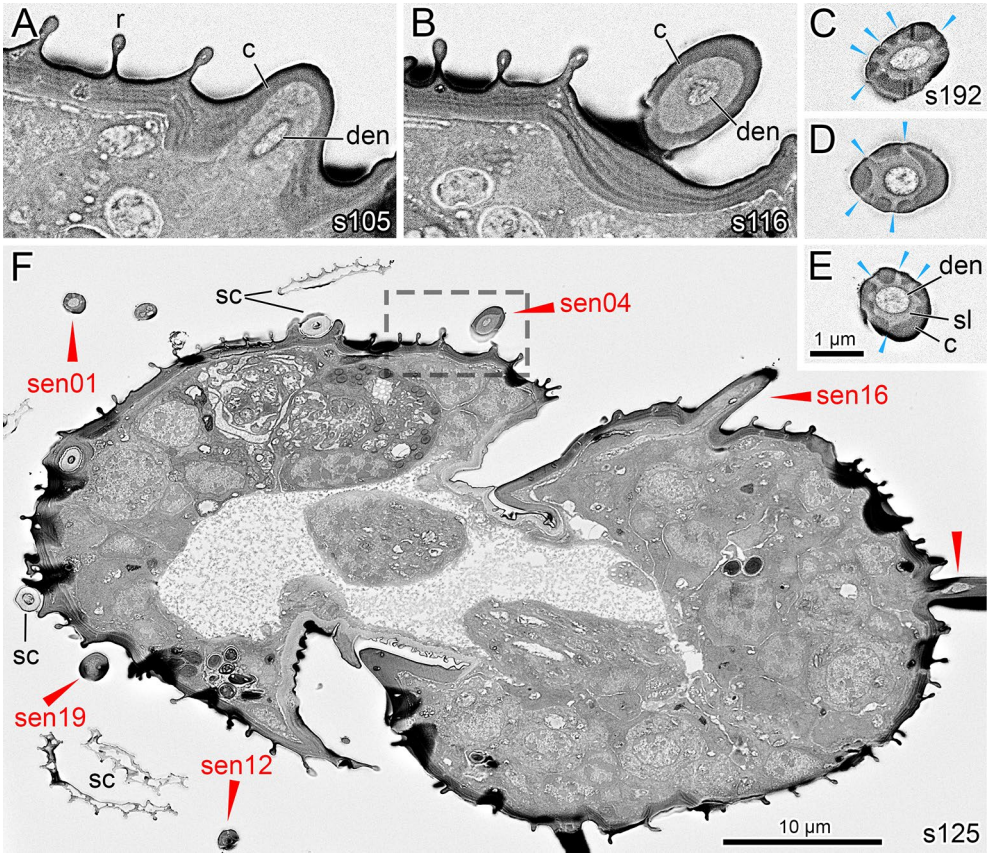

Fig. 5. Serial section scanning electron microscopic analysis of s. trichodea. Serial section images (Sects. 105, 116, and 192 from a complete series of 220) show the origin (**A**, **B**) and a more distal point (**C**) of a representative sensillum trichodeum. Sensilla trichodea were identified based on the absence of a socket at their point of origin (**A**) and the presence of a thick cuticle (c) with visible pores (blue arrowheads). A single dendrite (den) is located inside the sensillum. (r): ridge of the cuticule. (**D**, **E**): Cross-sections of two additional sensilla, each containing only one dendrite (den) surrounded by sensillum lymph (sl) and thick cuticule (**C**) with pores (blue arrowheads). (**F**) Cross-section of the antenna (Sect. 125, s125). All sensilla (indicated in the image with red arrowheads, sen 01–19) contained only a single dendrite. The boxed area contains sen04, which is also shown in panels A–C. sen01 and sen19 are also shown enlarged in different sections of the series in E and D, respectively. sc: scales of the antenna. The scale bar shown in E applies to images (**A**–**D**) as well.

frequency was calculated as the number of spikes during the stimulus time (0.5 s) minus the number of spikes before the stimulus onset (0.5 s) and expressed as the number of spikes. The response latencies were calculated based on the time difference between the stimulus onset and the first spike of the response, measured only where the response onset could be clearly identified.

Cross-adaptation

To determine whether the same or two different OSNs, located in the *s. trichodea,* can detect the two different compounds (E7,Z9-12Ac and Z7,Z9-12Ac), we performed a cross-adaptation experiment using the single sensillum setup. This experiment is based on the principle of neuronal adaptation. If a single neuron is responsible for detecting both compounds, after the first stimulus, which adapts the neuron, a reduced or abolished response to the second stimulus can be seen. In contrast, if two different neurons are involved, each will remain sensitive to its specific ligand, and a response to the second stimulus will still be observed[24,30,43]. The recording method was similar to that described in the single sensillum recordings paragraph. However, we used two stimuli for the two compounds to be positioned 1 cm apart, both directed into the continuous airflow. Each stimulus was controlled by two different stimulus controllers (CS-55, Ockenfels Syntech), using the same stimulus flow to deliver the odours independently. After establishing contact with the sensillum, the antenna was first stimulated with one compound for 500 ms, followed by a 100 ms inter-stimulus gap, and then stimulated again with either the same or the other compound for 500 ms. Four different combinations were tested: (1) first stimulus E7,Z9-12Ac, second stimulus E7,Z9-12Ac on 9 sensilla; (2) first stimulus E7,Z9-12Ac, second stimulus Z7,Z9-12Ac on 10 sensilla; (3) first stimulus Z7,Z9-12Ac, second stimulus Z7,Z9-12Ac on 7 sensilla and (4) first stimulus Z7,Z9-12Ac, second stimulus E7,Z9-12Ac on 9 sensilla. The position of the stimuli was randomised among replicates. The dose of the first and second tested compounds was 10^4 ng. The spikes were counted manually 0.5 s after each stimulus onset.

Serial section scanning electron microscopy

To examine the internal fine structure of sensilla trichodea type III, we performed serial section scanning electron microscopy (ssSEM). For serial ssSEM analysis, heads of male moths were removed from the body and fixed in 3% glutaraldehyde dissolved in 0.1 M phosphate buffer saline (pH 7.4) for 24 h at 4 °C. Then, a modified protocol of[44] was performed. After repeated rinses in 0.1 M phosphate buffer (pH 7.4; 30 min), samples were postfixed and contrasted in 1% osmium tetroxide reduced with 0.75% potassium ferrocyanide in phosphate buffer for 1 h. After extensive washes in distilled water (DW), samples were incubated in 1% aqueous uranyl-acetate in dark for 30 min. After DW washes, Walton's lead aspartate staining was performed at 60 °C for 8 min. The Walton's lead aspartate solution consisted of 0,066 g lead nitrate dissolved in 10 ml of aspartic acid stock solution. The stock solution was prepared by dissolving 0.998 g L-aspartic acid in 250 ml DW, then the pH was adjusted to 5.5 with 1 N KOH. After DW washes, the samples were dehydrated through an ascending concentration series of ethanol (30% 3 min, 50% 5 min, 70% 5 min, 90% 2 × 5 min, 100% 2 × 7 min), infiltrated with acetonitrile (2 × 7 min) and then with Durcupan (ACM; Fluka) overnight. The following day, the antennae were placed into silicon embedding moulds filled with Durcupan and heated at 60 °C for 24 h. Consecutive 100 nm-thick sections ($n \geq 250$) were cut from the resin-embedded antennae using a diamond knife (Diatome, Biel, Switzerland) mounted on an ultramicrotome (EM UC6, Leica, Wetzlar, Germany) and picked up on silicon wafers (Ted Pella). For imaging, we used a FEI Apreo field emission gun scanning electron microscope (Thermo Scientific) and a T1 column detector to record the backscattered electrons. The ssSEM micrographs were acquired with array tomography plugin in MAPs software (version: 3.23, ThermoFisher Scientific), which can facilitate the automatic acquisition of ssSEM images. The following imaging parameters were used: 4 mm working distance at high vacuum with 50 pA beam current, 2.27 kV high voltage, 3 or 4.5 µs/pixel dwell time, and 4 or 5.5 nm pixel size. The micrographs were 16384 × 12011 – 16384 pixels and we recorded 200–225 consecutive sections ($n = 3$ stacks from $n = 2$ moths). The ssSEM stacks were imported into Fiji TrakEM2 plugin for fine-alignment. The sensillar dendrites were annotated throughout consecutive serial sections using the IMOD (version 4.9) software package[45]. Only those sensilla with basal parts present in the ssSEM image stacks were included in the analysis. Among these, sensilla were identified as trichodea if they lacked a socket and were covered by a thick, porous cuticle[25]. Sensilla sectioned longitudinally were excluded from analysis, as their orientation makes dendrite reconstruction difficult.

Electroantennography

To assess which pheromone compounds can be detected by the whole male antenna instead of a single sensillum, we performed electroantennography (EAG) recordings. For the recordings, the antenna of the insect was excised and inserted into a glass capillary (ID 1.17 mm, Ockenfels Syntech) filled with Ringer solution[46] and attached to the reference silver electrode. The last (distal) segment of the antenna was cut and inserted into the recording glass electrode, which was also filled with Ringer solution. The antennal signal was 10 times pre-amplified, converted to a digital signal using a DC amplifier interface (IDAC-2, Ockenfels Syntech), and recorded with GC-EAD software (GC-EAD 2014, version 1.2.5, Ockenfels Syntech). Antennae were stimulated for 0.5 s using a stimulus controller (CS-55, Ockenfels Syntech). The stimulation air (1 L min^{-1}) was led into a constant, humidified and charcoal-filtered air stream (1 L min^{-1}). Synthetics of Z9-11Ac, Z9-12Ac, Z7,Z9-12Ac and E7,Z9-12Ac were tested in 10^1–10^4 ng doses on ten different male antennae ($n = 10$). A 20-s interval was maintained between consecutive stimulations to ensure that the antenna recovered fully and to minimise any adaptation effects from the previous compound. The solvent of the pheromone compounds (*n*-hexane) was used as a control stimulus. Absolute EAG amplitudes (mV) were used for data analysis.

Statistical analysis

All analyses were performed using R Statistical Software (version 4.3.0., R Core Team 2023). To compare responses to the control stimulus (*n*-hexane), raw data were used, and one-way ANOVA followed by Dunnett's post hoc test was conducted to select compounds that elicited significantly different responses from the control.

To account for differences in antennal sensitivity, spike counts (in the case of SSR) and absolute responses (in the case of EAG) were normalised to the response elicited by the control stimulus. Within each dose level, normalised responses were analysed using one-way ANOVA followed by Tukey's HSD post hoc test to determine which tested compounds differed from each other. To evaluate dose–response relationships for each compound, Spearman's rank correlation analyses were conducted between dose and the measured response (absolute response in EAG or spike number in SSR). Analyses were performed separately for each compound, and significance was evaluated using the *p*-values associated with the correlation coefficients.

Latencies were statistically evaluated only in the tuning specificity experiment (Fig. 1), and only for those components that elicited a significantly higher response than the control. For the other compounds, the onset and the first spike of the responses could not be clearly determined; therefore, the data were insufficient for statistical evaluation. For the active compounds, differences in latencies were assessed using one-way ANOVA followed by Tukey's HSD post hoc test.

For the cross-adaptation experiment, mean responses given to the first and second stimulus were compared using a paired *t*-test. Prior to statistical tests, data were examined for normality using the Shapiro–Wilk test. If Shapiro–Wilk indicated deviations from normality, data were further assessed using D'Agostino's test and visual inspection (e.g., Q-Q plots, histograms). The homogeneity of variance was tested using Levene's test. If necessary, $\log(x + 1)$ transformation was used to normalise the data. Outliers were defined as values exceeding 1.5 times the interquartile range above the third quartile or below the first quartile. All statistical tests were conducted at a significance level of $p < 0.05$.

Data availability

All data are presented in the manuscript and in the supplemental material.

Received: 2 June 2025; Accepted: 16 September 2025
Published online: 20 October 2025

References

1. Ioriatti, C. et al. Chemical ecology and management of *Lobesia botrana* (Lepidoptera: Tortricidae). *J. Econ. Entomol.* **104**, 1125–1137 (2011).
2. Vassiliou, V. A. Effectiveness of insecticides in controlling the first and second generations of the *Lobesia botrana* (Lepidoptera: Tortricidae) in table grapes. *J. Econ. Entomol.* **104**, 580–585 (2011).
3. Roelofs, W., Kochansky, J. & Cardé, R. Sex attractant of the grape vine moth, *Lobesia botrana*. *Mitteilungen der Schweizerischen Entomologischen Gesellschaft = Bulletin de la Société Entomologique Suisse Journal of the Swiss Entomological Society* **46**, 71 (1973).
4. Buser, H.-R., Rauscher, S. & Arn, H. Sex pheromone of *Lobesia botrana*: (E,Z)-7,9-dodecadienyl acetate in the female grape vine moth. *Zeitschrift für Naturforschung C* **29**, 781–783 (1974).
5. Arn, H., Rauscher, S., Guerin, P. & Buser, H.-R. Sex pheromone blends of three tortricid pests in European vineyards. *Agr. Ecosyst. Environ.* **21**, 111–117 (1988).
6. El-Sayed, A., Gödde, J., Witzgall, P. & Arn, H. Characterization of heromone blend for grapevine moth, *Lobesia botrana* by using flight track recording. *J. Chem. Ecol.* **25**, 389–400 (1999).
7. Witzgall, P. et al. New pheromone components of the grapevine moth *Lobesia botrana*. *J. Chem. Ecol.* **31**, 2923–2932 (2005).
8. Kaissling, K.-E. Physiology of pheromone reception in insects (an example of moths). *ANIR* **6**, 73–91 (2004).
9. Almaas, T. J. & Mustaparta, H. *Heliothis virescens*: Response characteristics of receptor neurons in sensilla trichodea type 1 and type 2. *J. Chem. Ecol.* **17**, 953–972 (1991).
10. Kurtovic, A., Widmer, A. & Dickson, B. J. A single class of olfactory neurons mediates behavioural responses to a *Drosophila* sex pheromone. *Nature* **446**, 542–546 (2007).
11. Koutroumpa, F. A. et al. Shifts in sensory neuron identity parallel differences in pheromone preference in the European corn borer. *Front. Ecol. Evol.* **2**, 65 (2014).
12. Vosshall, L. B., Wong, A. M. & Axel, R. An olfactory sensory map in the fly brain. *Cell* **102**, 147–159 (2000).
13. Dobritsa, A. A. et al. Integrating the molecular and cellular basis of odor coding in the *Drosophila* antenna. *Neuron* **37**, 827–841 (2003).
14. Couto, A. M. & Dickson, B. J. Molecular, anatomical, and functional organization of the *Drosophila* olfactory system. *Curr. Biol.* **15**, 1535–1547 (2005).
15. Hallem, E. A. & Carlson, J. R. Coding of odors by a receptor repertoire. *Cell* **125**, 143–160 (2006).
16. Zhang, D.-D. & Löfstedt, C. Moth pheromone receptors: Gene sequences, function, and evolution. *Front. Ecol. Evol.* **3**, 105 (2015).
17. Zhang, D.-D. & Löfstedt, C. Functional evolution of a multigene family: Orthologous and paralogous pheromone receptor genes in the turnip moth, Agrotis segetum. *PLoS ONE* **8**, e77345 (2013).
18. Nakagawa, T., Sakurai, T., Nishioka, T. & Touhara, K. Insect sex-pheromone signals mediated by specific combinations of olfactory receptors. *Science* **307**, 1638–1642 (2005).
19. Wanner, K. W. et al. Sex pheromone receptor specificity in the European corn borer moth, Ostrinia nubilalis. *PLoS ONE* **5**, e8685 (2010).
20. Miura, N., Nakagawa, T., Touhara, K. & Ishikawa, Y. Broadly and narrowly tuned odorant receptors are involved in female sex pheromone reception in Ostrinia moths. *Insect Biochem. Mol. Biol.* **40**, 64–73 (2010).
21. Montagné, N. et al. Functional characterization of a sex pheromone receptor in the pest moth Spodoptera littoralis by heterologous expression in Drosophila: Characterization of a moth sex pheromone receptor. *Eur. J. Neurosci.* **36**, 2588–2596 (2012).
22. Chang, H. et al. Sensillar expression and responses of olfactory receptors reveal different peripheral coding in two Helicoverpa species using the same pheromone components. *Sci. Rep.* **6**, 18742 (2016).
23. Liu, C., Liu, Y., Walker, W. B., Dong, S. & Wang, G. Identification and functional characterization of sex pheromone receptors in beet armyworm *Spodoptera exigua* (Hübner). *Insect Biochem. Mol. Biol.* **43**, 747–754 (2013).
24. Ammagarahalli, B. & Gemeno, C. Response profile of pheromone receptor neurons in male *Grapholita molesta* (Lepidoptera: Tortricidae). *J. Insect Physiol.* **71**, 128–136 (2014).
25. Godoy, R. et al. Antennal morphology and localization of a pheromone-binding protein of *Lobesia botrana* (Denis & Schiffermüller) (Lepidoptera: Tortricidae). *Neotrop. Entomol.* **48**, 422–432 (2019).
26. Pérez-Aparicio, A., Torres-Vila, L. & Gemeno, C. EAG responses of adult *Lobesia botrana* males and females collected from *Vitis vinifera* and *Daphne Gnidium* to larval host-plant volatiles and sex pheromone. *Insects* **10**, 281 (2019).
27. Cristofaro, A. et al. Olfactory cells responding to the main pheromone component and plant volatiles in *Lobesia botrana* (Den. & Schiff.): possible effects on monitoring systems. *IOBC/wprs Bull* **36**, 245–249 (2008).
28. Masante-Roca, I., Gadenne, C. & Anton, S. Three-dimensional antennal lobe atlas of male and female moths, *Lobesia botrana* (Lepidoptera: Tortricidae) and glomerular representation of plant volatiles in females. *J. Exp. Biol.* **208**, 1147–1159 (2005).
29. Arn, H. et al. Refining lepidoptera sex attractants. in 261–265 (Les Mediateurs chimiques, Versailles, 1981).
30. Takanashi, T. et al. Unusual response characteristics of pheromone-specific olfactory receptor neurons in the Asian corn borer moth, *Ostrinia furnacalis*. *J. Exp. Biol.* **209**, 4946–4956 (2006).
31. Wicher, D. Chapter Two - Olfactory Signaling in Insects. in *Progress in Molecular Biology and Translational Science* (ed. Glatz, R.) 37–54 (Academic Press, 2015).
32. Molnár, P. B. et al. Identification of the female-produced sex pheromone of an invasive greenhouse pest, the European pepper moth (Duponchelia fovealis). *J. Chem. Ecol.* **44**, 257–267 (2018).
33. Suresh, T., Roscoe, L. E. & Hillier, N. K. Pheromone and host plant odor detection in eastern spruce budworm, *Choristoneura fumiferana* Clemens (Lepidoptera: Tortricidae). *Insects* **14**, 653 (2023).
34. de Bruyne, M. & Baker, T. C. Odor detection in insects: Volatile codes. *J. Chem. Ecol.* **34**, 882–897 (2008).
35. Hansson, B. S. & Stensmyr, M. C. Evolution of insect olfaction. *Neuron* **72**, 698–711 (2011).
36. Renou, M. & Lucas, P. Sex pheromone reception in *Mamestra brassicae* L. (Lepidoptera): Responses of olfactory receptor neurones to minor components of the pheromone blend. *J. Insect Physiol.* **40**, 75–85 (1994).
37. Bäckman, A. C. et al. Antennal response of codling moth males, *Cydia pomonella* L. (Lepidoptera: Tortricidae), to the geometric isomers of codlemone and codlemone acetate. *J. Comp. Physiol. A* **186**, 513–519 (2000).
38. Zhang, J., Walker, W. B. & Wang, G. Pheromone reception in moths. in *Progress in Molecular Biology and Translational Science* 109–128 (Elsevier, 2015).
39. Baker, T. C., Domingue, M. J. & Myrick, A. J. Working range of stimulus flux transduction determines dendrite size and relative number of pheromone component receptor neurons in moths. *Chem. Senses* **37**, 299–313 (2012).
40. Ljungberg, H., Anderson, P. & Hansson, B. S. Physiology and morphology of pheromone-specific sensilla on the antennae of male and female *Spodoptera littoralis* (Lepidoptera: Noctuidae). *J. Insect Physiol.* **39**, 253–260 (1993).

41. Hallberg, E., Hansson, B. S. & Steinbrecht, R. A. Morphological characteristics of antennal sensilla in the European cornborer *Ostrinia nubilalis* (Lepidoptera: Pyralidae). *Tissue Cell* **26**, 489–502 (1994).
42. Nagy, B. Rearing of the European corn borer (*Ostrinia nubilalis* Hbn.) on a simplified artificial diet. *Acta Phytopathologica Academiae Scientiarum Hungaricae* **5**, 73–79 (1970).
43. Wu, H. et al. Specific olfactory neurons and glomeruli are associated to differences in behavioral responses to pheromone components between two Helicoverpa species. *Front. Behav. Neurosci.* **9**, 206 (2015).
44. Deerinck, T. et al. Enhancing serial block-face scanning electron microscopy to enable high resolution 3D nanohistology of cells and tissues. *Microsc. Microanal.* **16**, 1138–1139 (2010).
45. Kremer, J. R., Mastronarde, D. N. & McIntosh, J. R. Computer visualization of three-dimensional image data using IMOD. *J. Struct. Biol.* **116**, 71–76 (1996).
46. Ephrussi, B. & Beadle, G. W. Development of eye colors in Drosophila: Transplantation experiments on the interaction of vermilion with other eye colors. *Genetics* **22**, 65–75 (1936).
47. Roelofs, W., Kochansky, J., Cardé, R., Arn, H. & Rauscher, S. Sex attractant of the grape vine moth, *Lobesia botrana*. (1973).
48. Ando, T., Yoshida, S., Tatsuki, S. & Takahashi, N. Sex attractants for male Lepidoptera. *Agric. Biol. Chem.* **41**, 1485–1492 (1977).
49. Gray, T. G., Slessor, K. N., Shepherd, R. F., Grant, G. G. & Manville, J. F. European pine shoot moth, *Rhyacionia buoliana* (Lepidoptera: Tortricidae): Identification of additional pheromone components resulting in an improved lure. *Can. Entomol.* **116**, 1525–1532 (1984).
50. Arn, H., Rauscher, S., Buser, H.-R. & Guerin, P. M. Sex pheromone of *Eupoecilia ambiguella* female: analysis and male response to ternary blend. *J. Chem. Ecol.* **12**, 1417–1429 (1986).
51. Kinjo, N., Nagamine, M., Sugie, H. & Tamaki, Y. Sex pheromone of the sugarcane shoot borer, *Tetramoera schistaceana* Snellen (Lepidoptera: Tortricidae: Olethreutinae). Isolation and identification. *Jpn. J. Appl. Entomol. Zool.* **40**, 191–197 (1996).
52. McNair, C., Gries, G. & Gries, R. Sex pheromone components of *Enarmonia* formosana (Lepidoptera: Tortricidae). *Can. Entomol.* **131**, 85–92 (1999).
53. Rauscher, S., Arn, H. & Guerin, P. Effects of dodecyl acetate and Z-10-tridecenyl acetate on attraction of *Eupoecilia ambiguella* males to the main sex pheromone component, Z-9-Dodecenyl acetate. *J. Chem. Ecol.* **10**, 253–264 (1984).
54. Witzgall, P., Bengtsson, M. & Trimble, R. M. Sex pheromone of grape berry moth (Lepidoptera: Tortricidae). *Environ. Entomol.* **29**, 433–436 (2000).
55. Bjostad, L. B., Taschenberg, E. F. & Roelofs, W. L. Sex pheromone of the woodbine leafroller moth, Sparganothis sp. *J Chem Ecol* **6**, 797–804 (1980).

Acknowledgements

This study was supported by the National Research, Development and Innovation Office NKFIH K138128 and PD142628, and the Bolyai János Research Scholarship of Hungarian Academy of Sciences (JKJ). We thank the Electron Microscopy Center at the Institute of Experimental Medicine and S. Kőszegi for technical help with the FEI Apreo scanning electron microscope. The research was conducted using the Hungarian National Excellence Infrastructure Platform (KI 3-133-E)

Author contributions

Z.K.: experimental design, single sensillum recordings, writing the original draft; F.D.: insect rearing and experimental assistance; B.J.: electroantennographic recordings and data analysis; A.T.: electroantennographic recordings; A.F.: manuscript editing; J. F.: manuscript editing, financial support; V.T.: scanning electron microscopy, manuscript editing; G.K.; data analysis; G.N.; scanning electron microscopy, manuscript editing; J.J.: data and statistical analysis, visualisation, manuscript editing.

Funding

Hungarian National Excellence Infrastructure Platform, KI 3-133-E, KI 3-133-E, KI 3-133-E, KI 3-133-E, KI 3-133-E, KI 3-133-E, National Research, Development and Innovation Office, K138128 and PD142628, Bolyai János Research Scholarship of Hungarian Academy of Sciences, BO/00257/22.

Declarations

Competing interests

The authors declare they have no conflict of interest.

Ethical approval

No permits or approvals were required for the experiment on European grapevine moths (*Lobesia botrana*) in Hungary. After completing the experiment, we euthanised the animals by freezing them to avoid mixing with the natural population. During the preparation of the manuscript, we used Perplexity and ChatGPT (OpenAI) for language editing and improving the clarity of the text. All content was reviewed and revised by the authors, who take full responsibility for the final version.

Additional information

Supplementary Information The online version contains supplementary material available at https://doi.org/10.1038/s41598-025-20610-9.

Correspondence and requests for materials should be addressed to Z.K.